Geological Survey
of Canada

Current Research
2000-E6

Apparent formation-factor and porosity variation with pressure for Cretaceous shale of the Western Canada Sedimentary Basin, southern Alberta

T.J. Katsube, D.R. Issler, J. Loman, and W.C. Cox

2000

Natural Resources Canada Ressources naturelles Canada

Canada

©Her Majesty the Queen in Right of Canada, 2000
Catalogue No. M44-2000/E6E-IN
ISBN 0-660-18210-6

Available in Canada from the
Geological Survey of Canada Bookstore website at:
http://www.nrcan.gc.ca/gsc/bookstore (Toll-free: 1-888-252-4301)

A copy of this publication is also available for reference by depository libraries across Canada through access to the Depository Services Program's website at http://dsp-psd.pwgsc.gc.ca

Price subject to change without notice

All requests for permission to reproduce this work, in whole or in part, for purposes of commercial use, resale or redistribution shall be addressed to: Geoscience Information Division, Room 200, 601 Booth Street, Ottawa, Ontario K1A 0E8.

Authors' addresses

T.J. Katsube *(jkatsube@nrcan.gc.ca)*
Mineral Resources Division
Geological Survey of Canada
601 Booth Street
Ottawa, Ontario K1A 0E8

D.R. Issler *(dissler@nrcan.gc.ca)*
Natural Resources Canada
3303-33rd Street N.W.
Calgary, Alberta T2L 2A7

J. Loman *(jloman@ptslabs.com)*
PTS Labs International, Inc.,
4342 West 12 Street
Huston, Texas, U.S.A. 77055

W.C. Cox *(Wayne_Cox@pancanadian.ca)*
Pan Canadian Petroleum Ltd.
150-9th Avenue S.W.
Calgary, Alberta T2P 2S5

100-06730/

Apparent formation-factor and porosity variation with pressure for Cretaceous shale of the Western Canada Sedimentary Basin, southern Alberta

T.J. Katsube, D.R. Issler, J. Loman, and W.C. Cox
Mineral Resources Division, Ottawa

Katsube, T.J., Issler, D.R., Loman, J., and Cox, W.C., 2000: Apparent formation-factor and porosity variation with pressure for Cretaceous shale of the Western Canada Sedimentary Basin, southern Alberta; Geological Survey of Canada, Current Research 2000-E6; 6 p. (online; http://www.nrcan.gc.ca/gsc/bookstore)

Abstract: Ten shale samples from several Cretaceous stratigraphic units (Colorado Group) of the Western Canada Sedimentary Basin were obtained for determination of effective porosity (ϕ_E) and apparent formation-factor (F_a) as a function of confining pressure (P_c). These samples are part of a study to investigate the possibility that shale petrophysical property changes, in response to unloading by erosion of overburden, have contributed to the development of subhydrostatic pressures within the Cretaceous succession of the basin.

Results indicate that ϕ_E (0.9–13%) and F_a values (200–3800) at different confining pressures (P_c: 0–65 MPa) show trends that are typical of shale, with ϕ_E decreasing and F_a increasing with increased P_c; however, one sample from a siderite concretion unexpectedly displays a reverse F_a-P_c relationship. There are subtle indications that increased pore compressibility may be associated with abnormally pressured shale. These data form the basis for detailed analysis and interpretation in forthcoming studies.

Résumé : Dix échantillons de shale provenant de plusieurs unités stratigraphiques du Crétacé (Groupe de Colorado) dans le Bassin sédimentaire de l'Ouest du Canada ont été prélevés à des fins de détermination de la porosité efficace (ϕ_E) et du facteur de formation apparent (F_a) en fonction de la pression de confinement (P_c). Ces échantillons ont été recueillis dans le cadre d'une étude de la possibilité que les changements des propriétés pétrophysiques du shale, en réponse à un allégement de la charge résultant de l'érosion de la couverture de dépôts meubles, aient contribué à l'accumulation de pressions subhydrostatiques à l'intérieur de la succession crétacée du bassin.

Les résultats indiquent que les valeurs pour ϕ_E (de 0,9 à 13 %) et F_a (de 200 à 3 800) à différentes pressions de confinement (P_c : de 0 à 65 MPa) présentent des tendances typiques de celles observées pour les shales, soient une ϕ_E décroissante et un F_a croissant pour une P_c croissante. Cependant, pour un échantillon d'une concrétion de sidérite, on observe de manière inattendue une relation F_a-P_c inverse. Il y a de subtiles indications qu'une compressibilité accrue des pores puisse être associée aux shales soumis à des pressions anormales. Ces données constitueront les assises d'une analyse et d'une interprétation détaillées à venir.

INTRODUCTION

Economically important deposits of oil and gas are hosted within sandstones of the Viking Formation which is part of the shale-dominated Cretaceous Colorado Group of the Western Canada Sedimentary Basin. Much of the gas occurs within underpressured reservoirs and the reasons for this are poorly known. One possibility is that the shale has dilated in response to unloading during erosion and that they are drawing in fluids from the adjacent sandstones (e.g. Tóth and Corbet, 1986; Corbet and Bethke, 1992). Petrophysical measurements on Colorado shale samples were undertaken to investigate the possibility that shale physical property changes may have contributed to the development of subhydrostatic pressures within the Cretaceous succession of the Western Canada Sedimentary Basin (W.C. Cox, unpub. minutes of meeting, October 1995).

Ten shale samples from several stratigraphic units of the Cretaceous Colorado Group (undifferentiated upper ColoradoGroup and Second White Specks, Belle Fourche, and Westgate formations; Table 1) in the southern Alberta portion of the Western Canada Sedimentary Basin were obtained for determination of effective porosity (ϕ_E) and apparent formation-factor (F_a) as a function of confining pressure (P_c). Seven of these samples are from the Westgate Formation which overlies the Viking Formation. These ten samples are a subset of a larger suite of Colorado shale core samples that were selected for petrophysical and geochemical measurements (Katsube et al., 1998). In this paper, the methods of investigation are described and the results of the measurements are presented. Detailed analysis and interpretation of the data are planned for presentation in forthcoming papers.

METHOD OF INVESTIGATION

Sample collection and preparation

Ten cylindrical plugs of 2.54 cm (1 inch) diameter were cored in the vertical direction (parallel to core axis and perpendicular to bedding) from 10.16 cm (4 inch) split core samples. These plugs were cut into 0.5 to 1.0 cm thick discs for ϕ_E and F_a measurements under variable confining pressures. The plugs were collected from cores at depths close to where rock fragments were previously collected for mercury and helium porosimetry (Katsube et al., 1998; results summarized *in* Table 1). The exact depth position of plug samples depended on the quality of the core. Eight of the ten core plugs for this study were collected within 1 m or less of the previously investigated rock fragments; however, sample plugs SCD-P01 and SAF-P01 were collected 2 m and 2.8 m, respectively, below samples SCD-03 and SAF-02 (Table 1).

Table 1. Petrophysical characteristics of ten Cretaceous shale core samples from the Western Canada Sedimentary Basin (Katsube et al., 1998) that were selected for measurements of effective porosity (ϕ_E) and apparent formation-factor (F_a) as a function of confining pressure (P_c).

Sample no.*	Formation	h_s (km)	ϕ (%)	A (m^2/g)	d_m (nm)	P_g (kPa/m)
CRB-02	SWS	0.57	12.4–19.4	18.8	12.6	9.0–9.5
ACD-3R	SWS	0.56	7.8–8.3	13.3	7.9	7.0–7.5
ACD-17	WG	0.63	11.3–13.6	14.8	20.0	7.0–7.5
BEI-01	UC	0.58	5.5–8.4	13.1	5.0	4.5–5.0
BSR-12	WG	1.26	6.5–6.9	9.7	7.9	3.5–4.0
SCD-03	WG	2.10	6.9–15.1	11.5	7.9	6.5–7.0
MPD-01	WG	1.00	4.6–4.8	4.6	20.0	6.0–6.5
SAF-02	WG	2.51	6.1–9.0	9.4	7.9	10.5–11.0
EFR-01	WG	2.77	1.9–4.8	9.2	3.2	11.0–11.5
GBR-01	WG	2.54	3.0–6.8	12.1	7.9	12.0–12.5

*= Although identical sample numbers are used in Tables 2 and 3, there can be as much as a 2.8 m offset between the samples listed in this table and those listed in the others. This offset is less 1.0 m for most samples, except for SCD-P01 (2 m) and SAF-P01 (2.8 m).

Formation Group abbreviations: SWS – Second White Specs Formation. WG – Westgate Formation; UC – undifferentiated upper Colorado Group;

h_s = Current depth (km) from which the sample was obtained
ϕ = Porosity range for ϕ_{He}, ϕ_{Hg1} and ϕ_{Hg2}
ϕ_{He} = Effective porosity determined by helium porosimetry
ϕ_{Hg1} = Effective porosity determined by mercury porosimetry (pore sizes <10 μm)
ϕ_{Hg2} = Effective porosity determined by mercury porosimetry (pore sizes <250 μm)
A = Pore surface area determined by mercury porosimetry
d_m = Mode of nano-pore size distribution
P_g = Pressure gradient in Viking Formation (*from* Katsube et al., 1998)

Preparation for apparent formation-factor measurements

The ϕ_E-P_c and F_a-P_c measurements and the sample preparation procedures generally follow those described by Loman et al. (1993). These descriptions are partially repeated here. Upon arrival at the K & A Laboratories (Tulsa, Oklahoma, U.S.A.), the samples were fully cleaned using methylene chloride as the solvent. These samples were then oven dried for 48 hours at a temperature of 105°C (220°F). This was followed by cooling in desiccators. Subsequent to this, helium porosities were determined by first using a Boyles' Law double-celled helium porosimeter to obtain grain volume. Then the bulk volume of the samples was obtained by using the mercury immersion (Archimedes principle) technique. These measurements and procedures generally follow the recommended practices of the American Petroleum Institute (American Petroleum Institute, 1960), and further details of these measurements and procedures are described elsewhere (Loman et al., 1993).

Following the standard core analysis measurements, the samples were vacuum saturated with a test brine consisting of 80 000 ppm sodium chloride plus 20 000 ppm calcium chloride dihydrate (Loman et al., 1993). Subsequent to saturation, each sample was placed in individual electrically isolated core holders and flushed with brine using backpressures to insure 100% brine saturation.

Apparent formation-factor and porosity versus pressure measurements

Bulk electrical resistivities, ρ_b, were measured at multiple confining pressures between 3.5 and 65.6 MPa (500–9500 psi), at a frequency of 1000 Hz (Loman et al., 1993), using a Hewlett Packard Model 4276A LCZ meter. The samples were tested in a two-electrode system using a stainless steel electrode and end piece assembly. As confining pressure was increased, the amount of brine squeezed out of the sample was volumetrically measured and used to determine the porosity value at each of the confining pressures. The temperature variance was approximately ±1.1°C during the electrical resistivity tests. The apparent formation-factor, F_a, is determined using the following equation (Archie, 1942):

$$F_a = \frac{\rho_b}{\rho_w} \tag{1}$$

where ρ_w is the pore fluid resistivity. These F_a values include the effect of pore-surface conductivity (Wyllie and Spangler, 1952; Walsh and Brace, 1984), and do not represent the true formation-factor, F, values represented by

$$F = \frac{\tau^2}{\phi_c} \tag{2}$$

where ϕ_c is the connecting porosity (effective porosity minus storage porosity) and τ is the true tortuosity of the fluid-flow paths (Katsube and Williamson, 1994). Connecting porosity values can be determined by analyzing mercury intrusion and extrusion curves. The F values for these samples will be determined in a subsequent study using these F_a data.

EXPERIMENTAL RESULTS

Results of the ϕ_E-P_c and F_a-P_c measurements for the 10 shale samples are listed in Table 2 and these data are plotted in Figures 1 and 2, respectively. The ϕ_E and F_a values vary between 0.85–12.7% and 195–3770, respectively, and they are within the ranges previously reported for shale samples (ϕ_E = 0.3–12.2% and F_a = 99–5600: Loman et al., 1993; Katsube and Williamson, 1994, 1998; Katsube et al., 1996). For all samples, ϕ_E decreases with increasing P_c (Fig. 1) and, except for sample MPD-01, F_a increases with increasing P_c (Fig. 2). Depending on the initial porosity, ϕ_E shows an absolute decrease of 0.25–3.5% over the P_c range of 3.5–65 MPa (Table 2). Sample MPD-01 is from a siderite concretion and it differs significantly from the other samples in having a low porosity (< 5%) and a small pore surface area relative to its present depth of burial (Table 1). For comparison, other Westgate shale samples collected within a few metres of MPD-01 yield porosity values of 11–14% (Katsube et al., 1998). Also, the ϕ_E values for sample SCD-03 are low in comparison to previous measurements obtained by other methods (Table 1), and this requires a follow-up examination.

Table 3 summarizes the experimental results in terms of the fractional change in both ϕ_E and F_a over a specified pressure range. The parameter, $\Delta\phi_E$, is the ratio of ϕ_E measured at 6.9 MPa to the ϕ_E value at 62.1 MPa. Similarly, ΔF_a represents the ratio of F_a values at these two pressures. These pressure values were selected somewhat arbitrarily to minimize any possible errors associated with the lowest and highest P_c values used in the experiments. Table 3 also contains pressure gradient (P_g) data for the Viking Formation for the wells from which the samples were collected (Katsube et al., 1998). Figure 3 shows $\Delta\phi_E$ values plotted with respect to these Viking Formation pressure gradients. Normal formation pressure gradients for the Western Canada Sedimentary Basin are within the range, 9.5–10.2 kPa/m. Samples EFR-01 and GBR-01 are from wells where the Viking Formation is overpressured (>11 kPa/m) and they have the lowest ΔF_a values (0.49 and 0.51) and the highest $\Delta\phi_E$ values (2.2 and 1.6). Samples BEI-01 and BSR-12 are from regions where the Viking Formation is significantly underpressured (<5 kPa/m) and they are characterized by low ΔF_a values (<0.6) but moderate $\Delta\phi_E$ values (1.2–1.3).

DISCUSSION AND CONCLUSIONS

The ϕ_E-P_c (Fig. 1) and F_a-P_c (Fig. 2) data display values and trends that are typical for normal shale (Loman et al., 1993; Katsube and Williamson, 1994, 1998; Katsube et al., 1996), with ϕ_E decreasing and F_a increasing with increased P_c; however, for unknown reasons, sample MPD-01, a siderite concretion,

shows an unexpected decrease in F_a with increased P_c (Fig. 2). These unusual textural characteristics may be related its unique diagenetic history and its relatively high pyrite content (5 wt %). A plot of $\Delta\phi_E$ versus pressure gradient within the underlying Viking Formation (Fig. 3) does not show any distinct trend but there is a tendency for $\Delta\phi_E$ values to show a minimum at P_g values of 7–10 kPa/m. Samples from regions where the Viking Formation is presently overpressured (11–12.5 kPa/m) have high $\Delta\phi_E$ (1.6–2.2) and low ΔF_a (~0.5) values. Samples from areas where the Viking Formation is substantially underpressured (<5 kPa/m) also have low ΔF_a values (<0.6) but only moderate $\Delta\phi_E$ values (1.2–1.3). This suggests that overpressured shale may have a higher pore compressibility than normally pressured shale. The shale and clay mineral composition may also affect the behaviour of these samples; however, the full significance of these result await more detailed analysis and interpretation.

Table 2. Effective porostiy (ϕ_E) and apparent-formation-factor (F_{a1}) values as a function of confining pressure (P_c) for shale samples from the southern Alberta part of the Western Canada Sedimentary Basin. The pore fluid resistivity (ρ_w) was 0.0843 Ω·m (22.4°C).

Sample Formation	h (km)	k_a (μD)	P_c (MPa)	ϕ_E (%)	F_a
SCD-03	2.10	0.219	3.5	1.1	2695
(SCD-PO1)			6.9	1.1	2733
[Westgate			13.8	1.0	2826
Formation]			24.5	0.99	2941
			34.5	0.95	3093
			51.7	0.90	3251
			62.1	0.85	3323
			65.6	0.85	3335
BSR-12	1.26	1.42	3.5	4.6	270
(BSR-PO1)			6.9	4.4	320
[Westgate			13.8	4.1	396
Formation]			24.5	3.9	498
			34.5	3.8	494
			51.7	3.6	534
			62.1	3.5	553
			65.6	3.5	561
ACD-17	0.63	1.59	3.5	5.1	1542
(ACD-PO5)			6.9	5.0	1548
[Westgate			13.8	4.9	1599
Formation]			24.5	4.8	1681
			34.5	4.7	1749
			51.7	4.7	1807
			62.1	4.6	1847
			65.6	4.6	1880
MPD-01	1.00	1.05	3.5	5.1	3768
(MPD-PO1)			6.9	4.5	2962
[Westgate			13.8	4.3	2590
Formation]			24.5	3.9	2106
			34.5	3.6	1854
			51.7	3.2	1549
			62.1	3.0	1474
			65.6	2.8	1474
EFR-01	2.77	1.25	3.5	5.5	600
(EFR-PO1)			6.9	4.9	646
[Westgate			13.8	4.3	736
Formation]			24.5	3.3	864
			34.5	3.0	1011
			51.7	2.3	1199
			62.1	2.2	1314
			65.6	2.0	1379

Sample Formation	h (km)	k_a (μD)	P_c (MPa)	ϕ_E (%)	F_a
GBR-01	2.54	1.27	3.5	6.7	367
(GBR-PO1)			6.9	5.9	412
[Westgate			13.8	4.9	479
Formation]			24.5	4.4	556
			34.5	4.1	632
			51.7	3.9	741
			62.1	3.7	806
			65.6	3.6	855
SAF-02	2.51	0.50	3.5	4.4	547
(SAF-PO1)			6.9	4.3	553
[Westgate			13.8	4.2	576
Formation]			24.5	4.0	609
			34.5	3.8	650
			51.7	3.7	689
			62.1	3.5	730
			65.6	3.5	738
BEI-01	0.58	1.68	3.5	8.7	209
(BEI-PO1)			6.9	8.0	223
[Undifferentiated			13.8	7.5	253
Upper Colorado			24.5	7.4	326
Group]			34.5	7.2	372
			51.7	6.8	409
			62.1	6.6	447
			65.6	6.3	477
ACD-3R	0.56	2.27	3.5	5.2	195
(ACD-PO1)			6.9	5.2	201
[Second White			13.8	5.0	214
Specs]			24.5	4.6	238
			34.5	4.6	272
			51.7	4.4	301
			62.1	4.2	317
			65.6	4.1	336
CRB-02	0.57		3.5	12.7	217
(CRB-PO1)			6.9	12.1	224
[Second White			13.8	11.8	239
Specs]			24.5	11.5	258
			34.5	11.2	278
			51.7	10.9	307
			62.1	10.6	320
			65.6	10.2	335

h = Depth; k_a = Gas permeability; P_c = Confining pressure; ϕ_E = Effective porosity; F_a = Apparent formation-factor

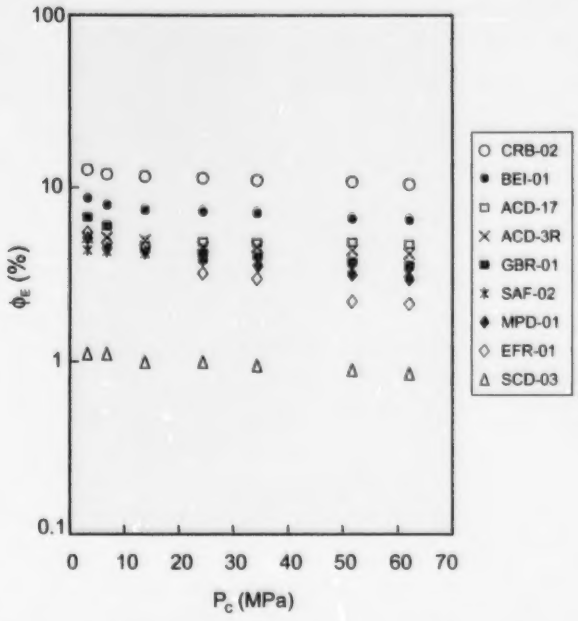

Figure 1. *Effective porosity (ϕ_E) versus confining pressure (P_c) for nine Cretaceous shale samples from the southern Alberta portion of the Western Canada Sedimentary Basin.*

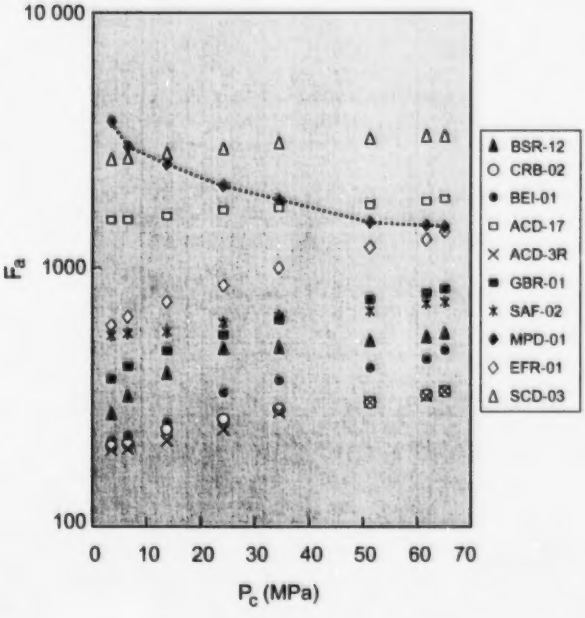

Figure 2. *Apparent formation-factor (F_a) versus confining pressure (P_c) for ten Cretaceous shale samples from the southern Alberta portion of the Western Canada Sedimentary Basin. Note the anomalous decrease in F_a with pressure for sample MPD-01 (dashed curve).*

Table 3. Effective porosity (ϕ_E) and apparent formation-factor (F_a) characteristics of the ten shale samples analyzed in this study.

Sample no.	Formation/ Group	h_s (km)	P_g (kPa/m)	$\Delta\phi_E$	ΔF_a
CRB-02	SWS	0.57	9.0–9.5	1.1	0.70
ACD-3R	SWS	0.56	7.0–7.5	1.2	0.63
ACD-17	WG	0.63	7.0–7.5	1.1	0.84
BEI-01	UC	0.58	4.5–5.0	1.2	0.50
BSR-12	WG	1.26	3.5–4.0	1.3	0.58
SCD-03	WG	2.10	6.5–7.0	1.3	0.82
MPD-01	WG	1.00	6.0–6.5	1.5	2.00
SAF-02	WG	2.51	10.5–11.0	1.2	0.76
EFR-01	WG	2.77	11.0–11.5	2.2	0.49
GBR-01	WG	2.54	12.0–12.5	1.6	0.51

Formation/Group abbreviations:
SWS – Second White Specks Formation; WG – Westgate Formation; UC – undifferentiated Upper Colorado Group

h_s = Current depth (km) from which the sample was obtained
P_g = Pressure gradient in the underlying Viking Formation (*from* Katsube et al., 1998)
$\Delta\phi_E$ = Ratio of ϕ_E at P_c = 6.9 MPa over ϕ_E at P_c = 62.1 MPa
ΔF_a = Ratio of F_a at P_c = 6.9 MPa over F_a at P_c = 62.1 MPa
P_c = Confining pressure

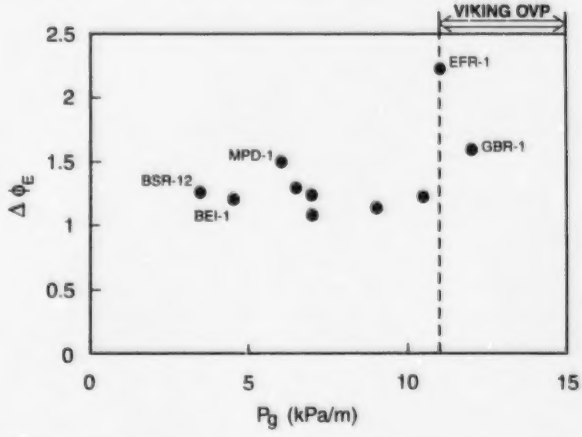

Figure 3. *Effective porosity variation ($\Delta\phi_E$) as a function of the pressure gradient (P_g) of the underlying Viking Formation (*from *Katsube et al., 1998). Note that samples from overpressured areas (>10.2 kPa/m) exhibit the largest changes in porosity under pressure. OVP = Overpressured zone of the Viking Formation.*

ACKNOWLEDGMENTS

The data used in this study were obtained as a result of a joint study between PanCanadian Petroleum Limited and the Geological Survey of Canada. The core samples used in this study were obtained from the Alberta Energy and Utility Board Core Research Center. The porosity and apparent formation-factor versus pressure measurements were performed at K&A Energy Consultants Inc. (Tulsa, Oklahoma). The authors

thank Dave Morrow (GSC-Calgary) for critically reviewing this paper and for his useful and constructive comments. The authors also thank S. Connell (Geological Survey of Canada, Ottawa) for her assistance in data compilation and presentation.

REFERENCES

American Petroleum Institute
1960: Recommended practice for core-analysis procedure; American Petroleum Institute, API Recommended Practice 40 (RP 40), First Edition, 55 p.

Archie, G.E.
1942: The electrical resistivity log as an aid in determining some reservoir characteristics; Transactions of the American Institute of Mining, Metallurgical and Petroleum Engineers, v. 146, p. 54–67.

Corbet, T.F. and Bethke, C.M.
1992: Disequilibrium fluid pressures and groundwater flow in the Western Canada Sedimentary Basin; Journal of Geophysical Research, v. 97, no. B5, p. 7203–7217.

Katsube, T.J. and Williamson, M.A.
1994: Effects of diagenesis on shale nano-pore structure and implications for sealing capacity; Clay Minerals, v. 29, p. 451–461.
1998: Shale petrophysical characteristics: permeability history of subsiding shales; *in* Shales and Mudstones II (ed.) J. Schieber, W. Zimmerle, and P.S. Sethi; Stuttgart, E. Schweizerbart'sche Verlagsbuchhandlung (Nägele u. Obermiller), p. 69–91.

Katsube, T.J., Cox, W.C., and Issler, D.R.
1998: Porosity characteristics of shale formations from the Western Canada Sedimentary Basin; *in* Current Research 1998-E; Geological Survey of Canada, p. 63–74.

Katsube, T.J., Issler, D.R., and Coyner, K.
1996: Petrophysical characteristics of shale from the Beaufort-Mackenzie Basin, northern Canada: permeability, formation factor, and porosity versus pressure; *in* Current Research 1996-B; Geological Survey of Canada, p. 45–50.

Loman, J.M., Katsube, T.J., Correia, J.M., and Williamson, M.A.
1993: Effect of compaction on porosity and formation factor for tight shales from the Scotian Shelf; *in* Current Research, Part E; Geological Survey of Canada, Paper 93-1E, p. 331–335.

Tóth, J. and Corbet, T.
1986: Post-Paleocene evolution of regional groundwater flow-systems and their relation to petroleum accumulations, Taber area, southern Alberta, Canada; Bulletin of Canadian Petroleum Geology, v. 34, no. 3, p. 339–363.

Walsh, J.B. and Brace, W.F.
1984: The effect of pressure on porosity and the transport properties of rocks; Journal of Geophysical Research, v. 89, p. 9425–9431.

Wyllie, M.R. and Spangler, M.B.
1952: Application of electrical resistivity measurements to problems of fluid flow in porous media; Bulletin of the American Association of Petroleum Geologists, v. 36, p. 359–403.

Geological Survey of Canada Project 870057